

Kondo effect versus indirect exchange in the two-impurity Anderson model: A Monte Carlo study

R. M. Fye and J. E. Hirsch

Department of Physics, University of California, San Diego, La Jolla, California 92093

D. J. Scalapino

Department of Physics, University of California, Santa Barbara, California 93106

(Received 14 November 1986)

The magnetic properties of two Anderson impurities in an electron gas are studied by use of a numerical simulation technique. It is found that magnetic correlations between impurities build up as the temperature is lowered up to roughly the Kondo temperature (T_K) and stay constant below T_K . The magnetic susceptibility is quenched on a temperature scale that depends sensitively on the relative size of T_K and the indirect exchange interaction. When the indirect exchange interaction is much smaller than the Kondo temperature all thermodynamic properties at low temperatures are indistinguishable from the ones obtained for a single-impurity model. The relation of these findings to other work on this problem is discussed.

I. INTRODUCTION

The properties of two magnetic impurities embedded in an electron gas have been a subject of considerable recent interest.¹⁻⁵ When the impurities are sufficiently far apart, they can be modeled by a single-impurity Anderson or Kondo Hamiltonian and the properties of such a system are well understood:⁶⁻⁸ the impurity and the surrounding conduction electrons develop correlations such that at sufficiently low temperatures the impurity moment is compensated by a "spin-compensation cloud" of surrounding conduction electrons, and the impurity susceptibility approaches a constant as $T \rightarrow 0$; the temperature scale over which the compensation occurs is given by the Kondo temperature T_K . When two impurities are close together, however, their spin-compensation clouds will overlap and interesting new effects appear due to the indirect exchange Ruderman-Kittel-Kasuya-Yosida (RKKY) interaction⁹ between the impurities.

A central question one would like to understand is how the competition between quenching of the individual moments and the RKKY interaction is resolved as the temperature is lowered. One expects the relevant energy scales to be the single-impurity Kondo temperature T_K and the strength of the RKKY interaction J . Different behavior should occur depending on whether T_K is larger, comparable or smaller than J . Jayaprakash, Krishnamurthy, and Wilkins have used perturbative scaling techniques to discuss the properties of two Kondo¹ and Anderson³ impurities in different asymptotic regimes. Their method, however, is not easily applicable to intermediate parameter regimes. For the case $J \ll T_K$, they conclude that the RKKY interaction plays a minor role and the impurities are individually quenched. A similar conclusion is reached in Ref. 2 using a functional-integral technique. On the other hand, Abrahams and Varma⁴ us-

ing higher-order perturbation theory and Jones and Varma⁵ using a numerical renormalization-group approach conclude that the RKKY interaction plays an important role at sufficiently low temperatures even for $J \ll T_K$.

The purpose of this paper is to establish some of the properties of the two-impurity Anderson model using a Monte Carlo method.¹⁰ With this approach it is difficult to achieve extreme regimes of parameters where the different scaling regimes can be clearly separated. However, for intermediate parameter regimes Monte Carlo simulations provide essentially exact results for this nontrivial many-body problem. It is precisely in this intermediate parameter regime where analytic approaches are most likely to fail or be inaccurate.

Our results show that the properties of the two-impurity system depend sensitively on the relative size of T_K and the RKKY interaction J . Abrahams and Varma as well as Jones and Varma have stressed that the impurities will retain "coherence" as $T \rightarrow 0$ even for the case $J < T_K$. Our results support this observation: as $T \rightarrow 0$, the impurity susceptibility goes to a constant (the moments are completely quenched), but the spin-spin correlation $\langle \sigma_1 \cdot \sigma_2 \rangle$ attains a finite nonzero value. However, we find that the two impurity spins never lock into a triplet state at $T \rightarrow 0$ in the ferromagnetic regime, i.e., $\langle \sigma_1 \cdot \sigma_2 \rangle < 1$ always. Despite the fact that we have studied an Anderson rather than a Kondo Hamiltonian, our results indicate that for both Hamiltonians the zero-temperature value of $\langle \sigma_1 \cdot \sigma_2 \rangle$ is a function of J/T_K and becomes very small for $J \ll T_K$. This will be discussed in detail later in the text. We also find that the uniform susceptibility is quenched on a temperature scale that decreases rapidly as J/T_K increases and approaches T_K for $J \ll T_K$; in contrast, the staggered susceptibility is always close to the isolated impurity values. Furthermore, we find that the local moment is somewhat enhanced by a ferromagnetic RKKY interaction relative to the isolated

impurity case and slightly suppressed when the RKKY interaction is antiferromagnetic. For cases where $J \ll T_K$, we find that the low-temperature thermodynamic properties of the two-impurity system are essentially identical to the ones of a single impurity system, in agreement with Refs. 1–3. We are not able to distinguish the different scaling regimes discussed in Ref. 1 for $J \gg T_K$, and are thus unable to check their predictions in that regime.

The paper is organized as follows. In Sec. II we define the Hamiltonian and discuss its properties in limiting cases. Section III briefly describes the numerical simulation method and gives some technical information. In Sec. IV we present and analyze the numerical results, and conclude in Sec. V with a discussion.

II. THE MODEL

We consider the two-impurity Anderson model¹¹ in the absence of direct hopping between impurities:

$$H = \sum_k \epsilon_k c_{k\sigma}^\dagger c_{k\sigma} + \sum_{k,\sigma} V_{ki} (c_{k\sigma}^\dagger d_{i\sigma} + \text{H.c.}) + \epsilon_d \sum_{\sigma} n_{d\sigma} + U \sum_{i=1,2} n_{di\uparrow} n_{di\downarrow}, \quad (1)$$

where $c_{k\sigma}$ and $d_{i\sigma}$ represent conduction electron operators and localized electron operators (d or f orbitals), respectively; the hybridization is taken to be

$$V_{ki} = V e^{ik \cdot R_i}. \quad (2)$$

We consider the case $\epsilon_d = -U/2$, which will give well-developed local moments at low temperatures. In the single impurity case, this choice ensures particle-hole symmetry if the conduction band is taken to be particle-hole symmetric, and the average occupation of the local level is unity. For two impurities, however, it is not possible to have particle-hole symmetry in general except for particular separations of the impurities. We choose a free-electron dispersion relation for the conduction electrons:

$$\epsilon_k = \frac{D}{2} \left[\left(\frac{k}{k_F} \right)^2 - 1 \right], \quad 0 \leq k \leq k_{\max} \quad (3)$$

and $k_{\max} = \sqrt{2}k_F$, so that the band extends from $-D/2$ to $D/2$.

The input for the Monte Carlo simulation is the Green's function for $U=0$, which is easily obtained from its equation of motion. Its components at the impurity sites (labeled 1 and 2) in imaginary frequencies are

$$g_{11}^0(i\omega_n) = g_{22}^0(i\omega_n) = \frac{1}{i\omega_n - \epsilon_d - F_0 - \frac{V^2 F_{12} F_{21}}{i\omega_n - \epsilon_d - F_0}}, \quad (4a)$$

$$g_{12}^0(i\omega_n) = g_{21}^0(i\omega_n) = \frac{V^2 F_{12}}{i\omega_n - \epsilon_d - F_0} g_{11}^0(i\omega_n), \quad (4b)$$

with

$$F_0 = \sum_n \frac{|V_{ki}|^2}{i\omega_n - \epsilon_k}, \quad (5a)$$

$$F_{12} = \sum_k \frac{e^{ik \cdot R}}{i\omega_n - \epsilon_k}. \quad (5b)$$

For the dispersion relation Eq. (3) we have

$$F_0 = \frac{\Delta D}{\pi} \int_0^{k_{\max}/k_F} dx \frac{x^2}{i\omega_n - \frac{D}{2}(x^2 - 1)}, \quad (6a)$$

$$F_{12} = \frac{\Delta D}{\pi k_F R^2} \int_0^{k_{\max}/k_F} dx \frac{x \sin[x(k_F R)]}{i\omega_n - \frac{D}{2}(x^2 - 1)}, \quad (6b)$$

$$\Delta = \pi V^2 \rho(\epsilon_F) = \frac{V^2 k_F^3}{2D}. \quad (6c)$$

Here we set $D=12$ and in the Monte Carlo simulations take parameters such that $D \gg U > \Delta$. In the free-electron limit, when $k_{\max} \rightarrow \infty$, F_{12} has the simple form

$$F_{12} = \frac{-\pi \rho(\epsilon_F)}{k_F R} e^{ik_F R [1 + (2i\omega_n/D)]^{1/2}}, \quad (7)$$

for $\omega_n \geq 0$ and $F_{12}(\omega_n) = F_{12}^*(-\omega_n)$. For large $k_F R$, $V^2 F_{12}$ is negligible and the Green's functions reduce to the ones of the single impurity case. When $k_F R$ is not large, F_{12} will give rise to an indirect exchange interaction between the impurities.

The usual RKKY calculation for the induced spin-spin interaction proceeds from a model in which an impurity spin S_i is coupled to the conduction electrons by

$$H = - \sum_{kk'} J^{sd} \psi_{k'} \left[\frac{\sigma}{2} \psi_k \right] \cdot S_i. \quad (8)$$

Using second-order perturbation theory in J^{sd} , the resulting RKKY exchange coupling J between two impurity spins

$$H = J(R) \mathbf{S}_1 \cdot \mathbf{S}_2, \quad (9)$$

separated by a distance R , is given by

$$J(R) = \frac{T}{2} \sum_n (J^{sd})^2 F_{12}(i\omega_n, k_F R). \quad (10)$$

In the free-electron case where F_{12} is given by Eq. (7), the low-temperature limit of Eq. (10) gives the usual RKKY result⁹

$$J = [J^{sd} \rho(\epsilon_F)]^2 \frac{\pi \epsilon_F \cos(2k_F R)}{2 (k_F R)^3}. \quad (11)$$

However, if J^{sd} is energy dependent, the structure of the RKKY interaction is modified near the impurity.^{12,13} Schrieffer and Wolf¹⁴ showed that for small values of Δ/U , the Anderson model could be transformed to a Kondo s - d exchange model with an energy-dependent antiferromagnetic s - d exchange interaction $J_{kk'}^{sd}$. For the case in which $\epsilon_d = -U/2$,

$$J_{kk'}^{sd} = V^2 \left[\frac{U}{\epsilon_k^2 - (U/2)^2} + \frac{U}{\epsilon_{k'}^2 - (U/2)^2} \right]. \quad (12)$$

For our present purposes, it is appropriate to replace ϵ_k and $\epsilon_{k'}$ by the energy transfer Matsubara frequency ω_n , so that Eq. (10) becomes

$$J = \left[\frac{8V^2}{U} \right]^2 \left[\frac{T}{2} \right] \sum_n \left[\frac{(U/2)^2}{\omega_n^2 + (U/2)^2} \right] F_{12}^2(i\omega_n, k_F R), \quad (13)$$

with $(8V^2/U)$, the effective Schrieffer-Wolf exchange coupling. Then, for example, in the free electron limit when $k_F R < D/U$,

$$J(R) \approx \left[\frac{8\Delta}{\pi U} \right]^2 \left[\frac{\pi}{4} \right]^2 U \frac{\cos(2k_F R)}{(k_F R)^2}. \quad (14)$$

Thus the dynamic response^{12,13} of the impurity Green's function changes with characteristic fall off of the interaction from $(k_F R)^{-3}$ to $(k_F R)^{-2}$ when $k_F R$ becomes smaller than of order D/U . For the parameters used in our Monte Carlo simulations, we are usually in the $k_F R < D/U$ regime, where $J(R) \sim (k_F R)^{-2}$.

In this paper we will use Monte Carlo techniques to calculate various physical observables such as the equal time spin-spin correlation function $\langle \sigma_1^z \sigma_2^z \rangle$ and the impurity susceptibilities. By studying the dependence of these quantities on the temperature and impurity separation $k_F R$, we can obtain insight into the behavior of the indirect exchange interaction. For the weak coupling case where Eq. (9) can be used we have for the spin-spin correlations, if we neglect charge fluctuations,

$$\langle \sigma_1^z \sigma_2^z \rangle = \frac{1 - e^{\beta J(R)}}{3 + e^{\beta J(R)}}. \quad (15)$$

We can take into account charge fluctuations to lowest order by renormalizing both the effective exchange and the spin-spin correlation by the local moment:

$$m^2 = \langle (\sigma_i^z)^2 \rangle = \langle (n_{i\uparrow} - n_{i\downarrow})^2 \rangle, \quad (16)$$

which will be less than unity for any finite U , and obtain

$$\langle \sigma_1^z \sigma_2^z \rangle = \frac{1 - e^{\beta J(R)m^2}}{3 + e^{\beta J(R)m^2}} m^2 \sim - \frac{\beta J(R)(m^2)^2}{4}, \quad (17)$$

for $\beta J(R)m^2 \ll 1$, and for the susceptibility

$$\chi = \frac{8\beta m^2}{e^{\beta J(R)m^2} + 3}. \quad (18)$$

If $J(R)$ remained fixed as the temperature decreases, a low-temperature singlet state would be formed when $J(R) > 0$ with $\langle \sigma_1^z \sigma_2^z \rangle$ going to $-m^2$ and χ vanishing as $8\beta m^2 e^{-\beta J(R)m^2}$. For $J(R) < 0$ (ferromagnetic coupling), the low-temperature limit of $\langle \sigma_1^z \sigma_2^z \rangle = m^2/3$ and $\chi \sim 8\beta m^2$. However, at low temperatures the spins become strongly correlated with the conduction electrons and the detailed behavior of $\langle \sigma_1^z \sigma_2^z \rangle$ and the susceptibility depends upon $J(R)/T_K$.

As Yosida and Yamada showed,¹⁵ perturbation theory in U/Δ can also provide a useful guide. For example, the equal time spin-spin correlation function to first order in U is given by

$$\langle \sigma_1^z \sigma_2^z \rangle = -2 \left[T \sum_l g_{12}^0(i\omega_l) \right]^2 + 4UT \sum_l \chi_{11}(i\omega_l) \chi_{21}(-i\omega_l), \quad (19)$$

with

$$\chi_{11}(i\omega_l) = T \sum_n g_{11}^0(i\omega_n + i\omega_l) g_{11}^0(i\omega_n), \quad (20a)$$

$$\chi_{22}(i\omega_l) = T \sum_n g_{21}^0(i\omega_n + i\omega_l) g_{12}^0(i\omega_n). \quad (20b)$$

In these expressions, the frequency dependence of g_{11}^0 is set by Δ . Therefore, when $k_F R < D/\Delta$, $\langle \sigma_1^z \sigma_2^z \rangle$ obtained from Eq. (19) decreases as $(k_F R)^{-2}$ due to the dynamics of the Anderson impurities, as previously discussed. We find in the next section that for $U/\pi\Delta \lesssim 1$, $\langle \sigma_1^z \sigma_2^z \rangle$ calculated from Eq. (19) is in reasonable agreement with our Monte Carlo data at intermediate temperature, while Eq. (17) gives better agreement for larger U .

III. MONTE CARLO METHOD

The input in the calculation is the imaginary-time Green's function for the noninteracting case:

$$g_{ij}^0(l, l') = T \sum_n e^{-i\omega_n \Delta \tau (l - l')} g_{ij}^0(i\omega_n). \quad (21)$$

Here, $i, j = 1, 2$ and $1 \leq l, l' \leq L$ label time slices of size $\Delta\tau$ with $\beta = L\Delta\tau$. The Green's functions $g_{ij}^0(i\omega_n)$ are given in Eq. (4).

An Ising variable $S_i(l)$ ($i = 1, 2$) is defined at every time slice for each impurity. A configuration is specified by these $2L$ Ising variables, and a Monte Carlo sweep involves attempting to flip each one of these variables sequentially. The Green's function for the fully interacting system for a given configuration obeys the Dyson equation:

$$g_\mu = g_\mu^0 + (g_\mu^0 - 1)(e^{V_\mu} - 1)g_\mu. \quad (22)$$

Equation (22) is a matrix equation where the matrix labels are impurity and time slice, i.e., $2L \times 2L$ matrices. μ labels electron spin. The potential V is diagonal in impurity indices and time indices and is given by

$$V_\mu(il; j'l') = \delta_{ij} \delta_{ll'} \mu \lambda S_i(l), \quad (23)$$

with $\mu = \pm 1$ and $\cosh \lambda = \exp(\Delta\tau U/2)$.

The Monte Carlo procedure used involves an exact updating of the fermion Green's function every time an Ising spin is flipped.^{10,16} The computer time for our case is proportional to $8L^3$ per sweep [$(nL)^3$ for n impurities]. The code is trivially vectorizable on a Cray computer since the updating do loop, which takes the bulk of the computer time, is very simple. A typical run of 6000 sweeps with $L = 64$ takes 16 min on a Cray XMP.

The only source of error in our computation (besides statistical) is the finite-time slice size $\Delta\tau$; we expect the systematic error to be proportional to $(\Delta\tau)^2 \Delta U$. We have performed the simulations for $\Delta = 0.5$ and $U = 2$ and 4 using $\Delta\tau = 0.25$ and 0.5. We find the differences with the two values of $\Delta\tau$ to be a few percent. We have also made extensive studies of the $\Delta\tau$ dependence in the single im-

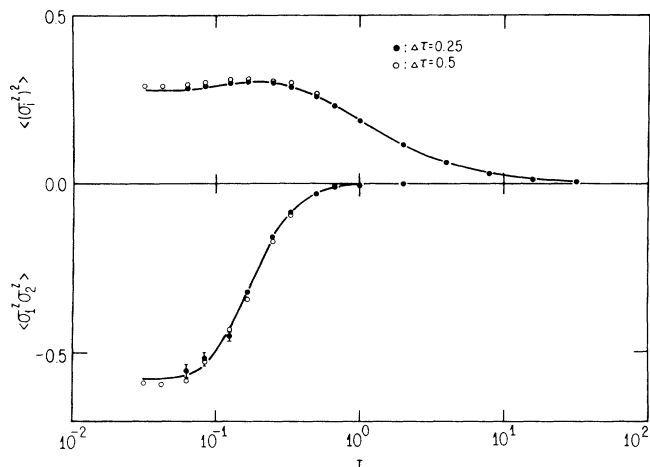


FIG. 1. Comparison of Monte Carlo and exact diagonalization results for local moment and spin-spin correlations for a two-impurity two-site conduction electron lattice. $U=2$, $\Delta=0.5$. Solid lines are exact results, solid and open circles Monte Carlo results for $\Delta\tau=0.25$ and $\Delta\tau=0.5$, respectively. The band is half-filled so that the impurity correlations on nearest-neighbor sites are antiferromagnetic.

purity case,¹⁷ and compared Monte Carlo results with exact diagonalization results for two impurities and a two-site conduction electron lattice. Figures 1 and 2 show comparison of exact and Monte Carlo results for the two-site model with $U=2$ and $\Delta=0.5$, for equal time correlations and susceptibilities [Eq. (25)]. It can be seen that the agreement is excellent ($\sim 5\%$ or better). We expect the results presented in the next section to have the same level of accuracy.

IV. NUMERICAL RESULTS

We start with a discussion of the indirect exchange interaction for intermediate values of the temperature. Fig-

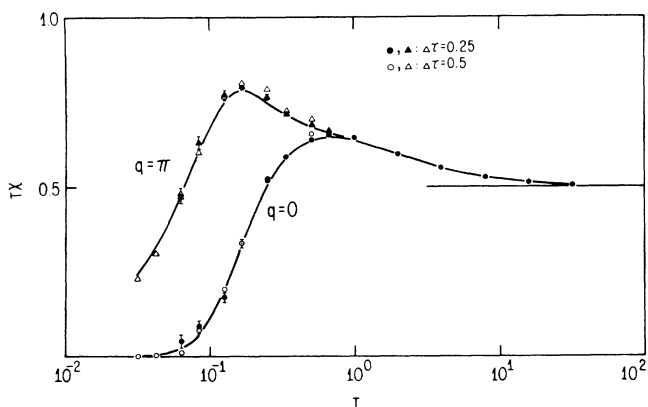


FIG. 2. Same as Fig. 1 for the susceptibilities. Solid and open circles denote uniform susceptibility, and solid and open triangles staggered susceptibility, for $\Delta\tau=0.25$ and 0.5 . Because the impurity correlations are antiferromagnetic, the staggered susceptibility is larger than the uniform one.

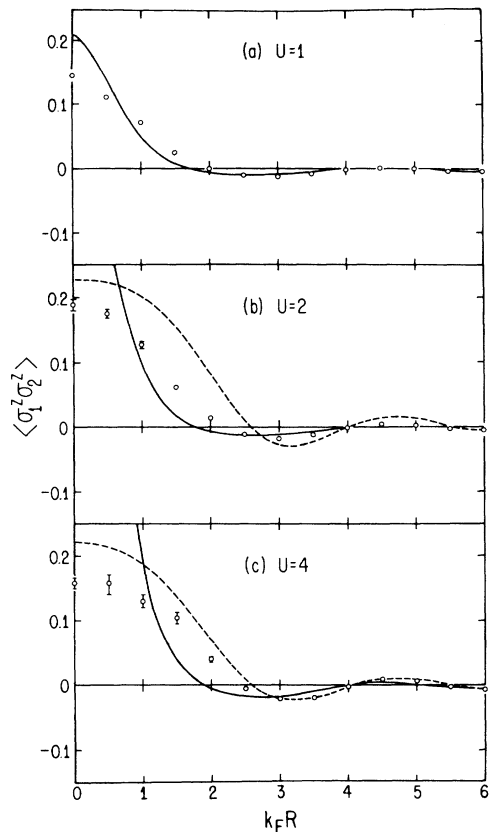
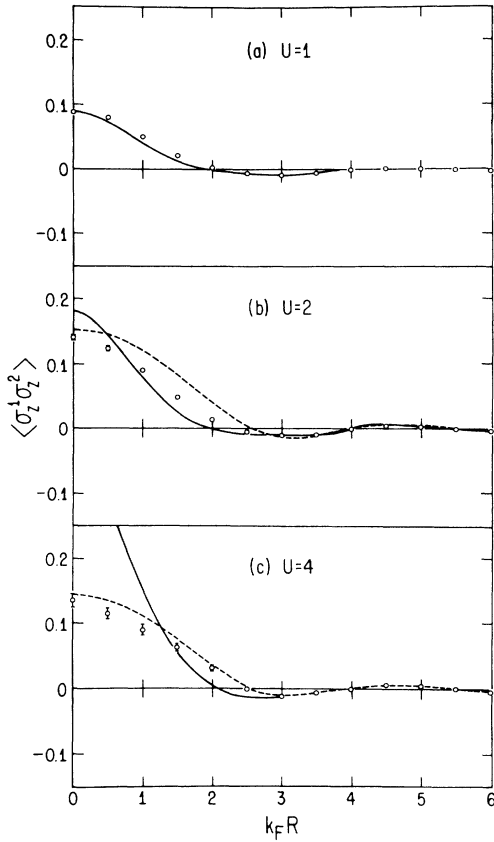
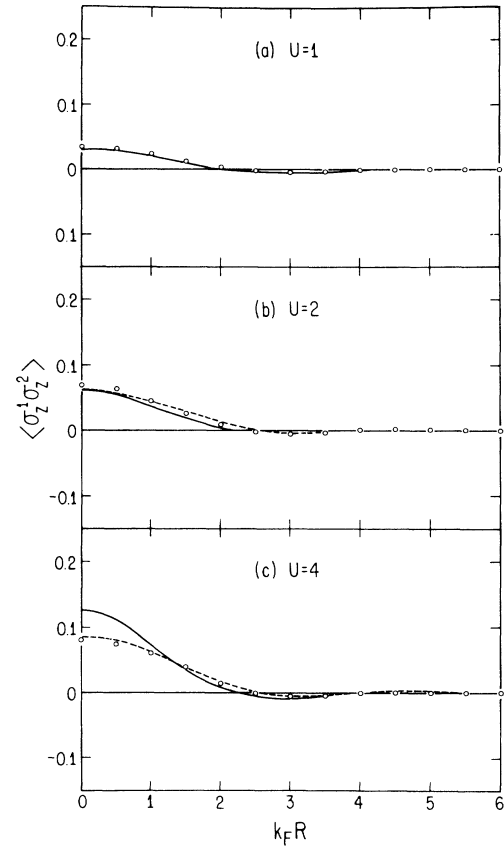


FIG. 3. Spin-spin correlations vs $k_F R$ for $\beta=4$. Solid lines are results from first-order perturbation theory, Eq. (19). The dashed lines are results from large- U perturbation theory equation (17).

ures 3 to 5 show results for spin-spin correlation versus distance for several values of U and $\beta=4, 8$, and 16 . It can be seen that the characteristic oscillatory behavior is obtained already for small values of U . The position of the first node in the indirect exchange interaction varies with U , beyond that the results are very similar for all values of U considered. The temperature dependence is found to be stronger for small values of U . It can be seen that our lowest-order perturbative expression Eq. (19) gives a reasonable fit to the data for $U=1$ at $\beta=4$ and $\beta=8$, but fails for $\beta=16$. Similarly, the large U expression Eq. (17) [with m^2 taken from the Monte Carlo results and $J(R)$ calculated from Eq. (13)] fits the data well for $U=4$ at $\beta=4$ and 8 , but not at $\beta=16$. The agreement of both expressions with the Monte Carlo data is not as good for $U=2$. The numerical results appear to follow a $1/R^2$ law in the range of $k_F R$ studied, as discussed in Sec. II. Figure 6 shows the U dependence of our results for $k_F R=0$, compared with the perturbative expressions. For $\beta=4$ and 8 , a smooth match of the weak- and strong-coupling perturbative expressions gives reasonable agreement with the numerical results for all U . For larger values of U , we expect the correlations to decay as $(\Delta/U)^2$ as predicted by the Schrieffer-Wolff transformation.

FIG. 4. Same as Fig. 3 for $\beta=8$.FIG. 5. Same as Fig. 3 for $\beta=16$.

Figures 7 to 12 show the temperature dependence of the local moment,

$$\langle \sigma_i^z \rangle = \langle (n_{di\uparrow} - n_{di\downarrow}) \rangle, \quad (24)$$

spin-spin correlations $\langle \sigma_1^z \sigma_2^z \rangle$, and uniform and staggered spin susceptibilities:

$$\chi = \int_0^\beta d\tau \langle [\sigma_1^z(\tau) + \sigma_2^z(\tau)][\sigma_1^z(0) + \sigma_2^z(0)] \rangle, \quad (25a)$$

$$\chi^{\text{st}} = \int_0^\beta d\tau \langle [\sigma_1^z(\tau) - \sigma_2^z(\tau)][\sigma_1^z(0) - \sigma_2^z(0)] \rangle, \quad (25b)$$

for $U=2$ and $k_F R=0.5, 1.0, 1.25, 1.5, 2.0,$ and 3.0 . We also show the results for the corresponding case with $k_F R = \infty$ for comparison, and the Kondo temperature for that case ($T_K=0.088$) as an arrow.

Consider Fig. 7. The exchange interaction is strongly ferromagnetic here; the local moment starts forming at high temperatures following the single impurity values but at low temperatures it is enhanced with respect to the $R = \infty$ case. At temperatures $\beta \sim 4$ to 8, the spin-spin correlations increase following roughly what one would get from just a spin-spin interaction term in the Hamiltonian:

$$\langle \sigma_1^z \sigma_2^z \rangle = \frac{1 - e^{-\beta J}}{3 + e^{-\beta J}} \sim \frac{-\beta J}{4}. \quad (26)$$

The dashed line in the figure show the temperature dependence of this expression, with $J=0.065$ fitted to the Monte Carlo results [it is slightly lower than that given by Eq. (13)]. At temperatures above $\beta=4$, the spin-spin correlations decrease below the value given by Eq. (26) due to charge fluctuations since the local moment is starting to decrease. At temperatures below $\beta=8$, the spin

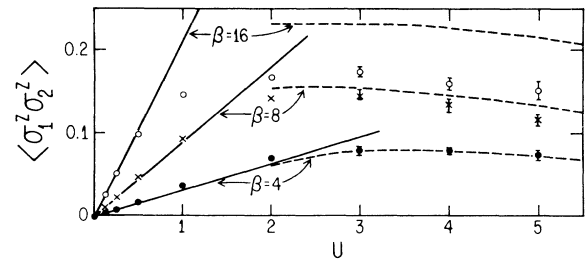


FIG. 6. Spin-spin correlations versus U for $k_F R=0$. Solid and dashed lines are results from first-order perturbation theory and large- U perturbation theory, respectively, Eqs. (19) and (17). The Monte Carlo results for $\beta=4, 8,$ and 16 are drawn as solid circles, crosses, and open circles, respectively.

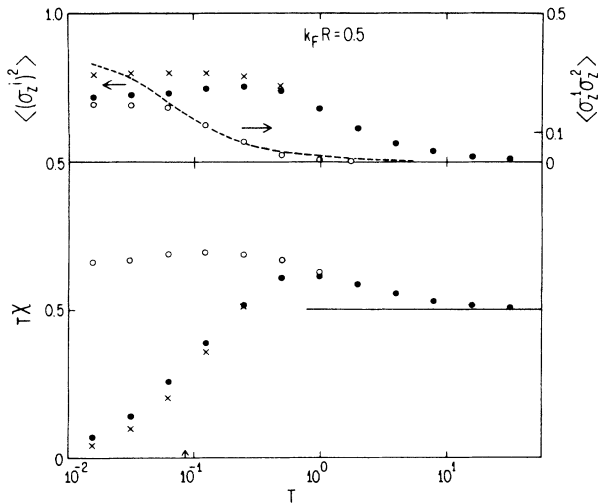


FIG. 7. Top: Spin correlations (open circles) and local moment (crosses) for two impurities, $k_F R = 0.5$, $U = 2$, and $\Delta = 0.5$ vs temperature. The solid circles show the local moment for $k_F R = \infty$. The dashed line shows the spin-spin correlations one would obtain from a temperature-independent indirect exchange interaction. Bottom: T times susceptibility for this case. Open circles, uniform susceptibility; crosses, staggered susceptibility; solid circles, susceptibility for $k_F R = \infty$.

correlations again deviate from Eq. (26), and appear to level off around $\beta = 32$. This suppression of the spin-spin correlations should not be attributed to charge fluctuations (the local moment is constant in this range), but rather to the fact that the Kondo effect is setting in and suppressing the RKKY interaction.

The susceptibility coincides with the single impurity values up to $\beta = 1$; for lower temperatures, $T\chi$ starts decreasing in the $R = \infty$ case due to the Kondo effect while

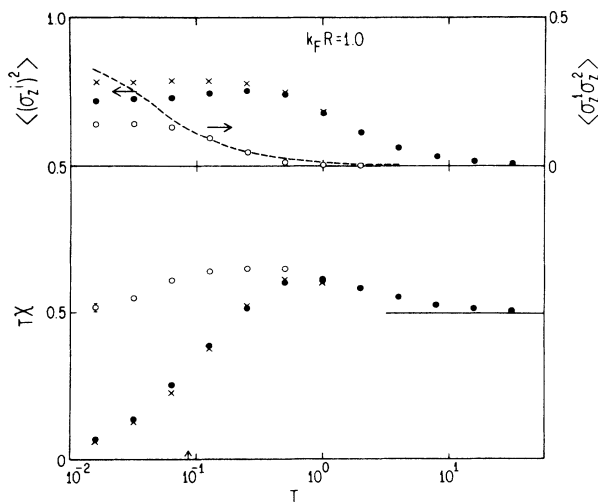


FIG. 8. Same as Fig. 7 for $k_F R = 1$.

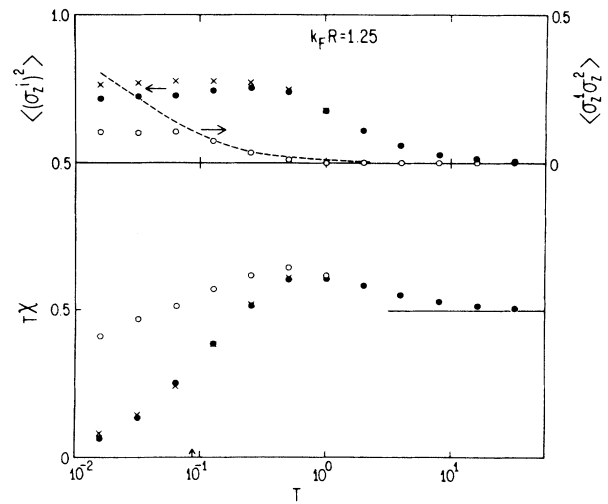


FIG. 9. Same as Fig. 7 for $k_F R = 1.25$.

it increases somewhat and then stays constant for the two impurities. We believe at lower temperatures $T\chi$ will be suppressed but have not reached that regime for this case. The staggered susceptibility shows values close to the single impurity ones but somewhat lower. This appears to be in disagreement to results obtained from a large- N expansion.¹⁸

As we increase the value of $k_F R$, we see in Figs. 8 to 12 that the spin-spin correlations become smaller since the indirect exchange interaction is decreasing. ($J = 0.05, 0.039, 0.024, 0.008, -0.006$ for $k_F R = 1, 1.25, 1.5, 2$, and 3 , respectively.) In all cases the spin-spin correlations follow an effective spin Hamiltonian behavior given by Eq. (26) and deviate from this when T approaches T_K . It is particularly clear in Figs. 9 and 10 that the spin-spin correlations have leveled off and will likely stay at this

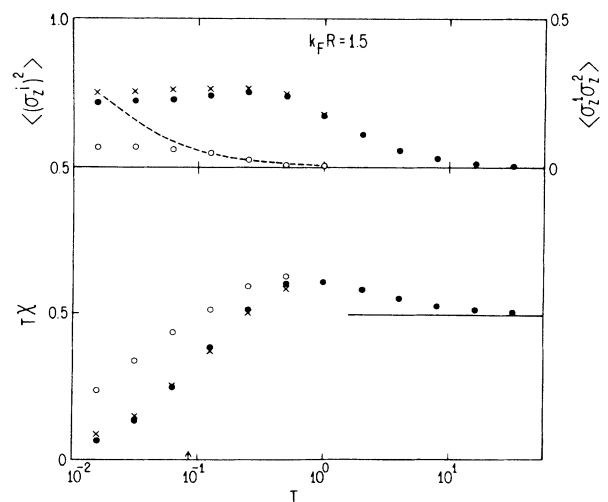
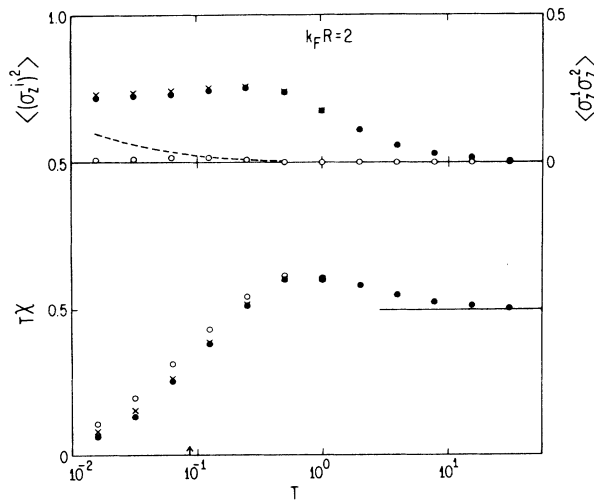
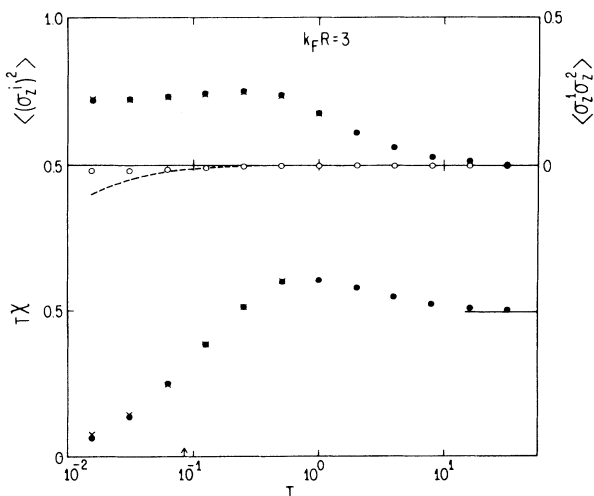
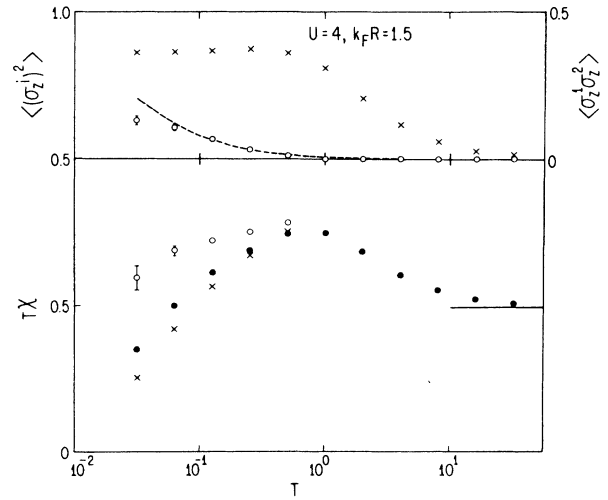


FIG. 10. Same as Fig. 7 for $k_F R = 1.5$.

FIG. 11. Same as Fig. 7 for $k_F R = 2$.

finite value, intermediate between 0 and $\frac{1}{3}$, down to $T=0$. Since in all cases the local moment is essentially the same while the asymptotic value of $\langle \sigma_z^1 \sigma_z^2 \rangle$ is quite different, it is clear that this asymptotic value is determined by the relation between the Kondo temperature and strength of the indirect exchange interaction rather than by charge fluctuations. Thus, we expect the same range of asymptotic values of $\langle \sigma_z^1 \sigma_z^2 \rangle$ to occur with the Kondo Hamiltonian (scaled by the local moment). The asymptotic value of $\langle \sigma_z^1 \sigma_z^2 \rangle$ is close to its value attained around the Kondo temperature.

As $k_F R$ increases and the indirect exchange becomes weaker we now see the susceptibility $T\chi$ starting to be suppressed in the temperature range studied. For $k_F R = 1.5$ and 2 it appears to follow a universal Kondo curve with a somewhat lower Kondo temperature. For smaller $k_F R$ it appears that the decay of $T\chi$ is slower

FIG. 12. Same as Fig. 7 for $k_F R = 3$.FIG. 13. Same as Fig. 7 for $U = 4$, $\Delta = 0.5$, and $k_F R = 1.5$.

than given by the simple single impurity behavior with a renormalized Kondo temperature. In all cases, single impurity behavior for all quantities is observed for $T \geq 1$.

Figure 12 shows an antiferromagnetic case ($k_F R = 3$). The spin-spin correlations appear to tend again to a finite nonzero value which is negative for this case. Here the staggered susceptibility is slightly larger than the uniform one. However, because the indirect exchange interaction is much smaller than the Kondo temperature there is not much difference with the single impurity results. The same was true in the weakly ferromagnetic case, Fig. 11.

Figure 13 shows one case for a larger U , $U = 4$. The local moment and susceptibilities are larger than for $U = 2$, but otherwise the results are qualitatively similar. The spin-spin correlations here follow the form Eq. (26) (with $J = 0.035$) over a wider temperature range because the energy scales Δ and T_K are more separated than in the previous case. But at sufficiently low T again they tend to level off.

V. DISCUSSION

We have presented results of Monte Carlo simulations for a two-impurity Anderson model which are essentially exact. We found the following features:

(a) At high temperatures ($T > \Delta$) the behavior is identical to isolated impurities. The local moment slowly develops as T is lowered below Δ , and the susceptibility is given roughly by $\chi \sim \langle \sigma_d^2 \rangle / T$. The spin-spin correlations are negligible.

(b) As T is lowered below Δ , the local moment is fully developed and levels off, while spin correlations start to grow. These are clearly induced by correlations between the impurity spins and the conduction electrons. For $U/\pi\Delta \lesssim 1$, the spin-spin correlations follow the behavior predicted by perturbation theory Eq. (19). For larger U , they are reasonably approximated by an effective spin Hamiltonian expression Eq. (9), with $J(R)$ the modified RKKY coupling given by Eq. (13) with the mean square local moment $\langle m^2 \rangle$ given by Eq. (16). At the same time

that spin correlations develop, the susceptibility starts to deviate from the single impurity behavior and to differ from the staggered susceptibility.

(c) As T is decreased further and approaches T_K the spin-spin correlations deviate from what one would obtain from a fixed indirect exchange J and start leveling off so that at low temperatures $\langle \sigma_1^z \sigma_2^z \rangle \sim J(R)/4T_K$. The local moment is essentially temperature independent in this range. One can interpret this as meaning that the indirect exchange interaction is *decreasing* proportionally to the temperature. The magnetic susceptibility $T\chi$ starts to decrease, but slower than the universal behavior of the single impurity (in the ferromagnetic regime).

(d) If the indirect exchange interaction is small compared to the Kondo temperature the impurities never develop significant correlations and all thermodynamic properties are essentially given by their single impurity values.

In summary, our results support the more conventional picture of the two-impurity problem rather than the one suggested in Refs. 4 and 5. For $J \ll T_K$, the impurities are independent and individually quenched; for J compa-

rable to T_K , the impurities develop magnetic correlations as T is lowered up to T_K and they are "collectively quenched," with the moments retaining residual correlations as $T \rightarrow 0$. Thus below T_K we find that $\langle \sigma_1^z \sigma_2^z \rangle$ does not approach the singlet -1 or triplet $\frac{1}{3}$ limit, rather it approaches an intermediate value of order $J(R)/4T_K$. These residual correlations may, in a concentrated system, be related to the low temperature coherence properties observed in heavy-fermion materials.¹⁹

ACKNOWLEDGMENTS

This work was started while one of us (J.H.) was visiting the Institute for Theoretical Physics, University of California, Santa Barbara. We are grateful to the participants in the workshop on "strongly interacting fermion systems" for providing a stimulating environment and for many discussions. Computations were performed at the Cray X-MP at the San Diego Supercomputer Center. The work was supported by the National Science Foundation under Grant No. PHY82-17853 supplemented by NASA, DMR-85-17756 and DMR-85-20481. J.H. is grateful to AT&T Bell Laboratories for financial support.

¹C. Jayaprakash, H. R. Krishnamurthy, and J. W. Wilkins, Phys. Rev. Lett. **47**, 737 (1981).

²S. Chakravarty and J. E. Hirsch, Phys. Rev. B **25**, 3273 (1982).

³C. Jayaprakash, H. R. Krishnamurthy, and J. W. Wilkins, J. Appl. Phys. **53**, 2142 (1982).

⁴E. Abrahams and C. M. Varma (unpublished).

⁵B. A. Jones and C. M. Varma (unpublished).

⁶K. G. Wilson, Rev. Mod. Phys. **47**, 773 (1975); H. R. Krishnamurthy, J. W. Wilkins, and K. G. Wilson, Phys. Rev. B **21**, 1003 (1980).

⁷N. Andrei, K. Furuya, and J. H. Lowenstein, Rev. Mod. Phys. **55**, 331 (1983).

⁸P. B. Wiegmann and A. M. Tsvetick, J. Phys. C **16**, 2281 (1983).

⁹M. A. Ruderman and C. Kittel, Phys. Rev. **96**, 99 (1954).

¹⁰J. E. Hirsch and R. M. Fye, Phys. Rev. Lett. **56**, 2521 (1986).

¹¹The model was introduced in the sixties and studied quite extensively using Hartree-Fock and low-order perturbation

theory. See for example, D. Kim and Y. Nagaoka, Prog. Theor. Phys. **30**, 743 (1963); S. Alexander and P. W. Anderson, Phys. Rev. **133**, A1594 (1964); P. Gottlieb and H. Suhl, Phys. Rev. **134A**, 1586 (1964); B. Caroli, J. Phys. Chem. Solids **28**, 1427 (1967).

¹²H. Ishii, Prog. Theor. Phys. **55**, 1373 (1976).

¹³A. M. Tsvetick, Zh. Eksp. Teor. Fiz. **76**, 2260 (1979) [Sov. Phys.—JETP **49**, 1142 (1979)].

¹⁴J. R. Schrieffer and P. A. Wolff, Phys. Rev. **149**, 491 (1966).

¹⁵K. Yosida and K. Yamada, Prog. Theor. Phys. **53**, 1286 (1975); K. Yamada, *ibid.* **53**, 970 (1975).

¹⁶R. Blankenbecler, D. J. Scalapino, and R. L. Sugar, Phys. Rev. D **24**, 2278 (1981).

¹⁷See Ref. 10 and R. M. Fye and J. E. Hirsch (unpublished).

¹⁸P. Coleman (private communication).

¹⁹C. M. Varma (private communication).